NASA/TM—2006-214354

Autonomous Navigation Error Propagation Assessment for Lunar Surface Mobility Applications

Bryan W. Welch and Joseph W. Connolly
Glenn Research Center, Cleveland, Ohio

May 2006

NASA STI Program . . . in Profile

Since its founding, NASA has been dedicated to the advancement of aeronautics and space science. The NASA Scientific and Technical Information (STI) program plays a key part in helping NASA maintain this important role.

The NASA STI Program operates under the auspices of the Agency Chief Information Officer. It collects, organizes, provides for archiving, and disseminates NASA's STI. The NASA STI program provides access to the NASA Aeronautics and Space Database and its public interface, the NASA Technical Reports Server, thus providing one of the largest collections of aeronautical and space science STI in the world. Results are published in both non-NASA channels and by NASA in the NASA STI Report Series, which includes the following report types:

- TECHNICAL PUBLICATION. Reports of completed research or a major significant phase of research that present the results of NASA programs and include extensive data or theoretical analysis. Includes compilations of significant scientific and technical data and information deemed to be of continuing reference value. NASA counterpart of peer-reviewed formal professional papers but has less stringent limitations on manuscript length and extent of graphic presentations.

- TECHNICAL MEMORANDUM. Scientific and technical findings that are preliminary or of specialized interest, e.g., quick release reports, working papers, and bibliographies that contain minimal annotation. Does not contain extensive analysis.

- CONTRACTOR REPORT. Scientific and technical findings by NASA-sponsored contractors and grantees.

- CONFERENCE PUBLICATION. Collected papers from scientific and technical conferences, symposia, seminars, or other meetings sponsored or cosponsored by NASA.

- SPECIAL PUBLICATION. Scientific, technical, or historical information from NASA programs, projects, and missions, often concerned with subjects having substantial public interest.

- TECHNICAL TRANSLATION. English-language translations of foreign scientific and technical material pertinent to NASA's mission.

Specialized services also include creating custom thesauri, building customized databases, organizing and publishing research results.

For more information about the NASA STI program, see the following:

- Access the NASA STI program home page at *http://www.sti.nasa.gov*

- E-mail your question via the Internet to *help@sti.nasa.gov*

- Fax your question to the NASA STI Help Desk at 301–621–0134

- Telephone the NASA STI Help Desk at 301–621–0390

- Write to:
  NASA STI Help Desk
  NASA Center for AeroSpace Information
  7121 Standard Drive
  Hanover, MD 21076–1320

NASA/TM—2006-214354

Autonomous Navigation Error Propagation Assessment for Lunar Surface Mobility Applications

Bryan W. Welch and Joseph W. Connolly
Glenn Research Center, Cleveland, Ohio

National Aeronautics and
Space Administration

Glenn Research Center
Cleveland, Ohio 44135

May 2006

This report is a formal draft or working paper, intended to solicit comments and ideas from a technical peer group.

This report contains preliminary findings, subject to revision as analysis proceeds.

Level of Review: This material has been technically reviewed by technical management.

Available from

NASA Center for Aerospace Information
7121 Standard Drive
Hanover, MD 21076–1320

National Technical Information Service
5285 Port Royal Road
Springfield, VA 22161

Available electronically at http://gltrs.grc.nasa.gov

Autonomous Navigation Error Propagation Assessment for Lunar Surface Mobility Applications

Bryan W. Welch and Joseph W. Connolly
National Aeronautics and Space Administration
Glenn Research Center
Cleveland, Ohio 44135

Abstract

The NASA Vision for Space Exploration is focused on the return of astronauts to the Moon (ref. 1). While navigation systems have already been proven in the Apollo missions to the moon, the current exploration campaign will involve more extensive and extended missions requiring new concepts for lunar navigation. In this document, the results of an autonomous navigation error propagation assessment are provided. The analysis is intended to be the baseline error propagation analysis for which Earth-based and Lunar-based radiometric data are added to compare these different architecture schemes, and quantify the benefits of an integrated approach, in how they can handle lunar surface mobility applications when near the Lunar South pole or on the Lunar Farside.

1. Introduction

In support of NASA's Vision for Space Exploration (ref. 1), error propagation of an autonomous navigation system is analyzed for multiple lunar surface mobility applications. This error propagation is conducted using Gaussian random errors as the errors associated with accelerometers and gyroscopes. In the Apollo era, lunar rovers used simple autonomous navigation systems to traverse the surface and return to the lunar module. The analysis provided in this document looks at two lunar surface mobility applications that model mobility applications, and determine the maximum error propagation that occurred due to the Gaussian random errors in the autonomous navigation system. This analysis is to be used as a starting point for future analysis which will include radiometric data (either from Earth-based assets or a Lunar-based constellation) to improve navigation performance.

2. Mission Design

Two lunar surface tracks are designed for the purposes of this analysis. The two tracks are quite different from each other in two ways: velocity profile and track route. Typically, lunar surface roving can be characterized by several stages such as:

1. Acceleration from lunar module
2. Traversing lunar surface to destination
3. Deceleration to stop at destination
4. Acceleration to lunar module
5. Traversing lunar surface to lunar module
6. Deceleration to stop at module

The first of the two surface roving applications takes a more simplistic approach to this surface roving profile, in that it eliminates the acceleration and deceleration profiles and keeps a constant velocity profile throughout the simulation.

Circular Constant Velocity Track

The first track that is created follows the outline of a small circle centered on the moon's fixed axis latitude/longitude point (0° N. 0 °E.). The radius of the circular track is 15 km on the lunar surface. Therefore, the rover would be at a maximum of 30 km away from the lunar module when at 180° rotation from the lunar module. The duration of the roving mission was set at 6 hr. The starting point of the track is placed at the point (0.496 °N. 0 °E.), corresponding to a 15 km radius.

This circular track is designed to have a constant velocity throughout the simulation. Since the track has a radius of 15 km and it takes 6 hr to traverse the track, the resulting speed the rover has is 4.375 m/s.

It is important to note that this constant speed track does not start with zero magnitude velocity, nor does it slow down, as a normal rover application would. This rover has a constant speed throughout the entire duration of the simulation. The only acceleration resulting from this profile is due to the track being circular.

Figure 1 provides an illustration of the circular track, which is created in Satellite Tool Kit (STK). Figure 1 illustrates the constant speed of the rover on this track by capturing images at 0, 0.75, 1.5, 2.25, 3, 3.75, 4.5, 5.25, and 6 hr after the starting point of the rover from the lunar module. Note that in the image bottom right region, representing the rover 6 hr after departure from the lunar module, the rover is again at the starting point.

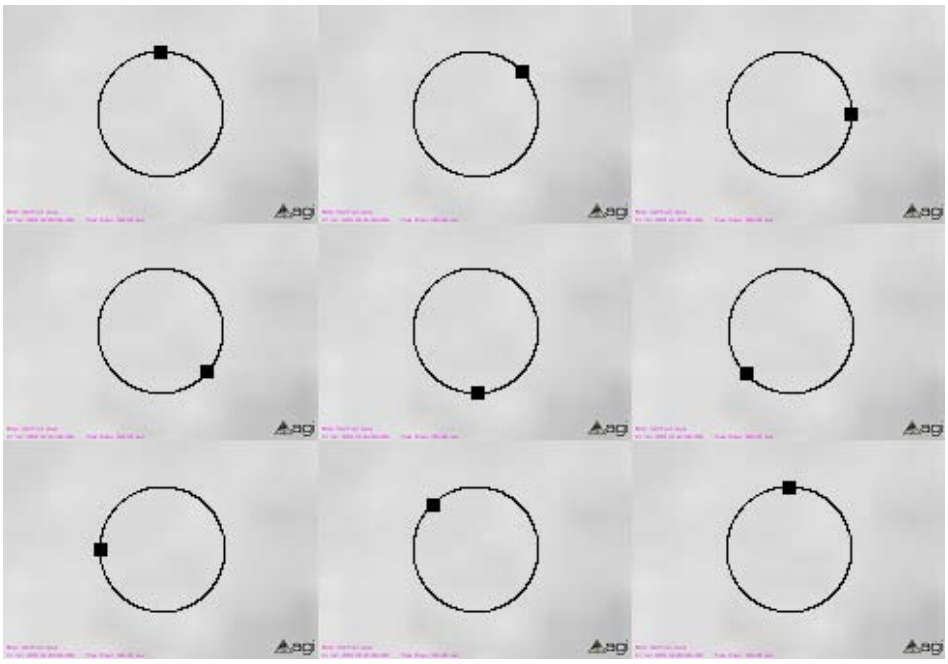

Figure 1.—Circular track velocity illustration.

Straight Variable Velocity Track

The second track that is created follows the outline of a line centered on the moon's fixed axis latitude/longitude point (0 °N. 0 °E.). The length of the straight track is 30 km on the lunar surface, which would be the farthest distance that the rover would be away from the lunar module before it returns. This is approximately the distances that the Apollo rovers traversed in the later missions. The duration of the roving mission is set at 6 hr, 3 hr for each traverse of the track. The starting point of the track is placed at the point (0 °N. –0.496 °E.) (–0.496 °E. corresponds to 15 km on the lunar surface from 0 °E.).

This straight track is designed to have a variable velocity throughout the simulation. Since the track has a length of 30 km and it takes 3 hr to traverse the track in one direction, the average velocity due east is 2.7778 m/s, but the track has a maximum velocity of 4.3771 m/s due east, due to the sinusoidal accelerations that are placed throughout the track.

It is important to understand that this variable velocity track starts with zero velocity, and ends with a zero velocity when it reaches its destination, as a normal rover application would. While the rover is traversing the track in each direction, it is constantly accelerating or decelerating. Therefore, the rover does not have a constant magnitude velocity at any point of the simulation. In fact, the magnitude of the velocity profile follows the shape of the first half of a sinusoid waveform.

Figure 2 provides an illustration of the straight track, which is created in Satellite Tool Kit (STK). Note that the simulation does not include any of the terrain information that is portrayed in the figure. Figure 2 attempts to illustrate the variable magnitude velocity nature of this track by capturing images of the track at 0, 0.75, 1.5, 2.25, 3, 3.75, 4.5, 5.25, and 6 hr after the starting point of the rover at the lunar module. Note that in the image bottom right region, representing the rover 6 hr after departure from the lunar module it returns to the starting point.

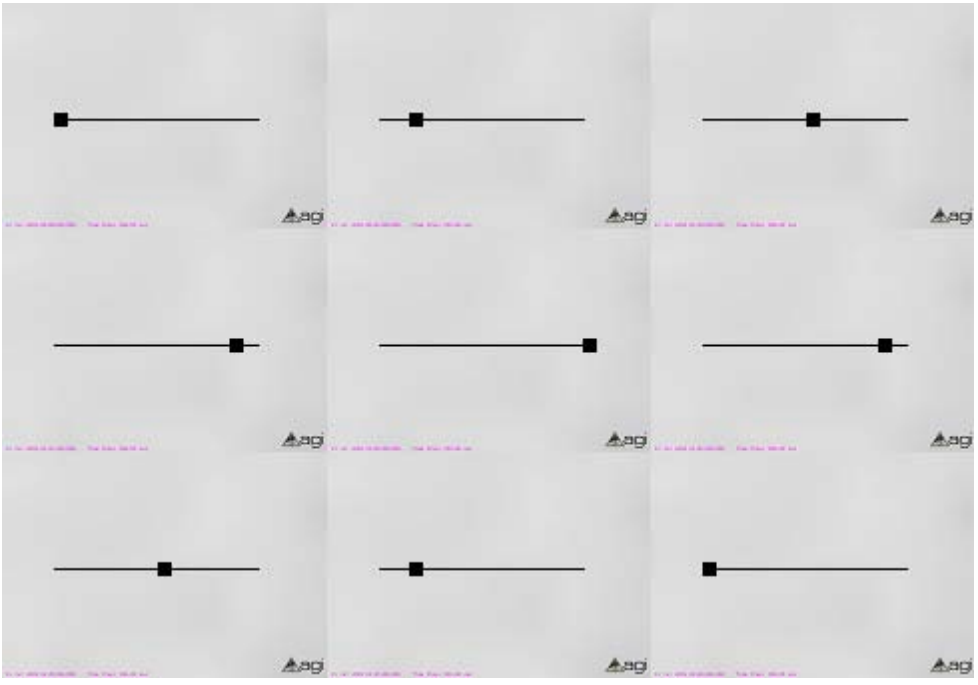

Figure 2.—Straight track velocity illustration.

3. Methodology

This analysis uses the two rover tracks discussed earlier with IMU sensor data to propagate errors throughout the roving mission to determine the total error at the end of the rover mission. The error propagation analysis is updated every simulated second throughout the 6 hr roving application simulation (ref. 2). There are 20 distinct noise histories for each track that are propagated using Matlab. At the end of simulation for each track, plots are created showing the error growth in the three local topocentric coordinates.

The basis for the error propagation simulation was derived in (ref. 2). Inputs to the simulation model include acceleration, case-to-inertial direction cosine matrix, and angular velocity. Outputs of the simulation are the same quantities corrupted by IMU errors. IMU errors can include the following:

Gyroscope bias drift
Gyroscope scale factor
Gyroscope non-orthogonality
Gyroscope random walk
Accelerometer bias repeatability
Accelerometer scale factor
Accelerometer non-orthogonality

Scale factor errors are the ratio of the input-to-output mapping for the gyroscope and accelerometer. Non-orthogonality errors arise because the actual gyroscope/accelerometer axes cannot be installed perfectly orthogonal to each other. In the gyroscope measurement Y_g in the simulation, the IMU has an additive error $\delta^I w_c^C$ consisting of the following:

$$Y_g = {}^I w_c^C + \delta^I w_c^C \tag{1}$$

$$\delta^I w_c^C = d_C + S_g {}^I w_c^C + \Gamma_g {}^I w_c^C + \varepsilon_w \tag{2}$$

where

${}^I w_c^C$ true angular velocity

d_C gyroscope bias drift

S_g gyroscope scale factor matrix

Γ_g gyroscope non-orthogonality matrix

ε_w gyroscope Gaussian white noise random walk

In the accelerometer Y_a measurement in the simulation, the IMU has an additive error δa_C consisting of the following:

$$Y_a = a_C + \delta a_C \tag{3}$$

$$\delta a_C = b_a + S_a a_C + \Gamma_a a_C + B_a a_C \tag{4}$$

where

a_C true acceleration

b_a accelerometer bias

S_a accelerometer scale factor matrix

Γ_a accelerometer non-orthogonality matrix

B_a gyroscope-to-accelerometer misalignment matrix

Now, if some of the parameters in equations (2) and (4) are rewritten as follows, equations (5) to (19), then equations (2) and (4) become equations (20) and (21). It is useful to have the parameters in these forms when computing the covariance of the IMU system. The equations for the covariance of the gyroscope and accelerometer errors are given in equations (22) and (23).

$$D\left({}^{I}w_c^C\right) = diag\left({}^{I}w_c^C\right) \tag{5}$$

$$s_g = \left[S_{gx}, S_{gy}, S_{gz}\right]^T \tag{6}$$

$$S_g\,{}^{I}w_c^C = D\left({}^{I}w_c^C\right)s_g \tag{7}$$

$$D\left(a_C\right) = diag\left(a_c\right) \tag{8}$$

$$s_a = \left[S_{ax}, S_{ay}, S_{az}\right]^T \tag{9}$$

$$S_a a_C = D\left(a_C\right)s_a \tag{10}$$

$$F\left({}^{I}w_c^C\right) = \begin{bmatrix} 0 & 0 & 0 \\ -{}^{I}w_{cx}^C & 0 & 0 \\ 0 & {}^{I}w_{cx}^C & -{}^{I}w_{cy}^C \end{bmatrix} \tag{11}$$

$$\gamma_g = \left[\Gamma_{gyz,}\, \Gamma_{gyz}, \Gamma_{gzx,}\right]^T \tag{12}$$

$$\Gamma_g\,{}^{I}w_c^C = F\left({}^{I}w_c^C\right)\gamma_g \tag{13}$$

$$F\left(a_C\right) = \begin{bmatrix} 0 & 0 & 0 \\ -a_x & 0 & 0 \\ 0 & a_x & a_y \end{bmatrix} \tag{14}$$

$$\gamma_a = \left[\Gamma_{ayz,}\, \Gamma_{azy}, \Gamma_{azx,}\right]^T \tag{15}$$

$$\Gamma_a a_C = F(a_C)\gamma_a \tag{16}$$

$$a_c^x = \begin{bmatrix} 0 & a_z & -a_y \\ -a_z & 0 & a_x \\ a_y & -a_x & 0 \end{bmatrix} \tag{17}$$

$$\beta_a = \left[B_{ax}, B_{ay}, B_{az}\right]^T \tag{18}$$

$$B_a a_C = -a_c^x \beta_a \tag{19}$$

$$\delta^I w_c^C = d_C + D\left(^I w_c^C\right)s_g + F\left(^I w_c^C\right)\gamma_g + \varepsilon_w \tag{20}$$

$$\delta a_C = b_a + D(a_C)s_a + F(a_C)\gamma_a - a_c^x \beta_a \tag{21}$$

$$P_{\delta wc} = {}^I w_c^C P_{\psi c}\, {}^I w_c^{C^T} + P_{dc} + D\left(^I w_c^C\right)P_{sg}D^T\left(^I w_c^C\right) + F\left(^I w_c^C\right) + P_{\gamma g}F^T\left(^I w_c^C\right) \tag{22}$$

$$P_{\delta ac} = P_{ba} + D(\delta a_C)P_{sa}D^T(\delta a_C) + F(\delta a_C)P_{\gamma a}F^T(\delta a_C) + a_c^x P_{\beta a} a_c^{x^T} \tag{23}$$

where

$P_{\delta wc}$ gyroscope error

$P_{\Psi c}$ angular error in case coordinates

P_{dc} gyroscope bias drift

P_{sg} gyroscope scale factor

$P_{\gamma g}$ gyroscope of the non-orthogonality

$P_{\delta ac}$ accelerometer error

P_{ba} accelerometer bias

P_{sa} accelerometer scale factor

$P_{\gamma a}$ accelerometer non-orthogonality

$P_{\beta a}$ gyroscope-to-accelerometer misalignment

4. IMU Parameters

The analysis performed in this document utilized the properties of an IMU model provided by James Russell Carpenter of NASA Goddard Space Flight Center (ref. 2). This IMU model contains gyroscopes and accelerometers. The best-case properties of the gyroscopes can be found in table 1, while the best-case properties of the accelerometers can be found in table 2. Additional parameters that were assumed for the simulations can be found in table 3.

TABLE 1.—GYROSCOPE BEST-CASE PROPERTIES

Standard deviation of bias drift	0.01°/hr
Standard deviation of scale factor	33 ppm
Power spectral density of random walk	0.01°/√(hr)

TABLE 2.—ACCELEROMETER BEST-CASE PROPERTIES

Standard deviation of bias repeatability	0.06 milli-g
Standard deviation of scale factor	100 ppm

TABLE 3.—ADDITIONAL PROPERTIES ASSUMED FOR ANALYSIS

Standard deviation of gyroscope non-orthogonality	0 ppm
Standard deviation of accelerometer non-orthogonality	0 ppm
Standard deviation of initial angular error	0 arcsec

5. Results

Circular Constant Velocity Track

The resulting error graph for the circular constant velocity track is shown in figure 3. There are three subplots in the figure, representing the topocentric x, y, and z dimensions as the rover traverses the track. Since the rover is known to be on the surface, the topocentric errors could also be converted to latitude and longitude errors. This would eliminate the error in altitude if one could utilize a detailed elevation map of the lunar surface. Reducing this one error could reduce the overall error that is experienced in a simulation run.

The unit for the error in any of the topocentric dimensions is kilometers. The maximum error experienced in any case for the circular constant magnitude of the velocity track in any of the dimensions is less than 4.5 km in the topocentric x dimension, 5.5 km in the topocentric y dimension, and 5 km in the topocentric z dimension.

Straight Variable Velocity Track

The resulting error graph for the straight variable velocity track is shown in figure 4. Again, there are three subplots in the figure, representing the topocentric x, y, and z dimensions as the rover traverses the track. Since the rover is known to be on the surface, the topocentric errors could also be converted to latitude and longitude errors. This would eliminate the error in altitude if one could utilize a detailed elevation map of the lunar surface. Reducing this one error could reduce the overall error that is experienced in a simulation run. The maximum error experienced in any case for the straight variable velocity track in any of the dimensions is less than 5.5 km in the topocentric x dimension, 4.5 km in the topocentric y dimension, and 4 km in the topocentric z dimension.

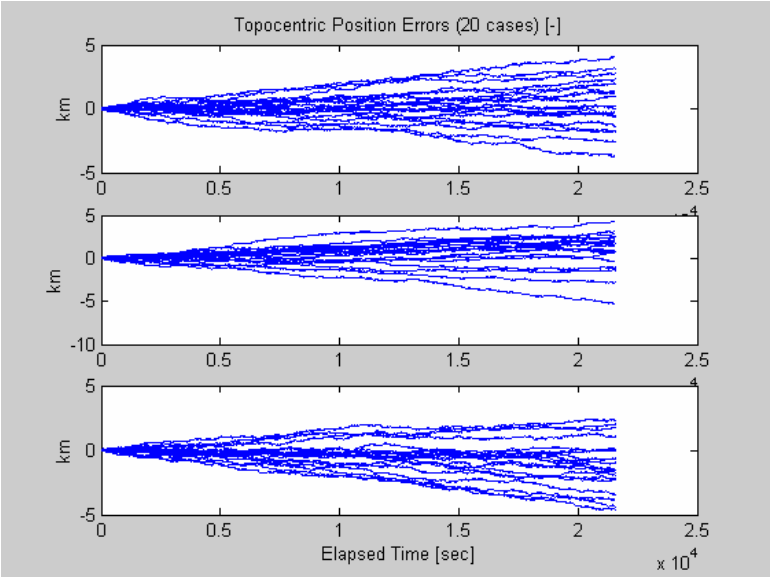

Figure 3.—Circular constant velocity results.

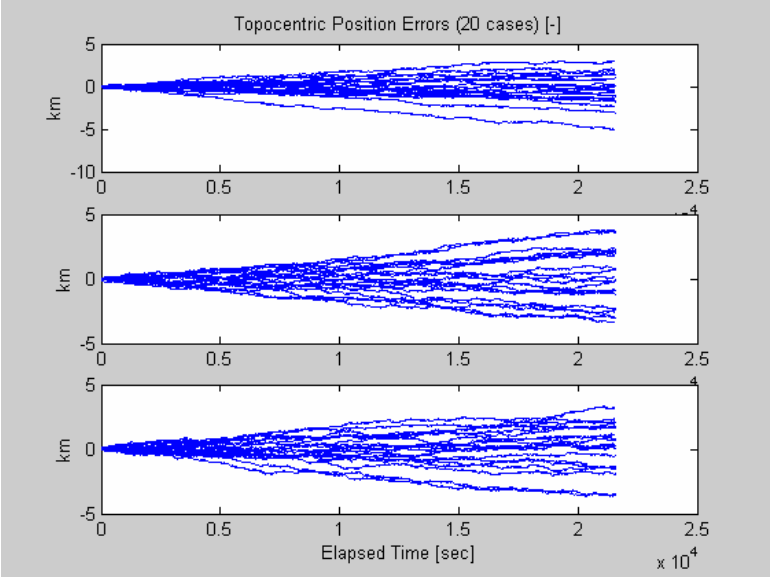

Figure 4.—Straight variable velocity results.

6. Conclusions

This analysis illustrates the error propagation that can occur on a lunar surface roving application when using an IMU that contains accelerometer and gyroscope biases and scale factor errors. This study is a first attempt to try and understand how these errors can affect performance of an IMU navigation system by creating two roving tracks with different traverse profiles and different magnitude velocity profiles. The study showed that it is possible to have errors up to 5 km in a single topocentric dimension. It is believed that the similar error propagation profiles are due to the nature of the rover traversing along

the spherical moon. When a similar analysis is done for lunar descent profiles to the surface, they have much different error propagation profiles (ref. 3). Using a combination of radiometric/IMU navigation system could reduce the error that is propagated, by closing the open-loop nature of the IMU system alone. Radiometric data would act as the feedback to make the radiometric/IMU navigation system a closed-loop system.

There are a few types of actions that a follow on study should contain to advance the work performed in this study, such as:

1. Create additional velocity profiles for these two track traverse profiles. This could include an acceleration/deceleration from a constant velocity.
2. Simulate additional IMU performance characteristics to determine which error sources are the most dominant.
3. Simulate these rover tracks with radiometric data from multiple lunar constellations to compare to IMU data alone.
4. Simulate these rover tracks with a combination of IMU data and radiometric data to compare to IMU data alone and radiometric data alone.

References

1. President Bush, George W., "Vision for Space Exploration," Presidential Action, Jan 2004.
2. IMU Model provided by James R. Carpenter, NASA Goddard Space Flight Center, email dialogue.
3. Carpenter, James R., "Strapdown IMU Error Model," Unpublished Manuscript, Oct. 2005.

REPORT DOCUMENTATION PAGE

Form Approved
OMB No. 0704-0188

1. AGENCY USE ONLY (*Leave blank*)	2. REPORT DATE	3. REPORT TYPE AND DATES COVERED
	May 2006	Technical Memorandum

4. TITLE AND SUBTITLE

Autonomous Navigation Error Propagation Assessment for Lunar Surface Mobility Applications

5. FUNDING NUMBERS

WBS 439432.07.04.03.01

6. AUTHOR(S)

Bryan W. Welch and Joseph W. Connolly

7. PERFORMING ORGANIZATION NAME(S) AND ADDRESS(ES)

National Aeronautics and Space Administration
John H. Glenn Research Center at Lewis Field
Cleveland, Ohio 44135–3191

8. PERFORMING ORGANIZATION REPORT NUMBER

E–15629

9. SPONSORING/MONITORING AGENCY NAME(S) AND ADDRESS(ES)

National Aeronautics and Space Administration
Washington, DC 20546–0001

10. SPONSORING/MONITORING AGENCY REPORT NUMBER

NASA TM—2006-214354

11. SUPPLEMENTARY NOTES

Responsible person, Bryan W. Welch, organization code RCI, 216–433–3390.

12a. DISTRIBUTION/AVAILABILITY STATEMENT

Unclassified - Unlimited
Subject Category: 17

Available electronically at http://gltrs.grc.nasa.gov

This publication is available from the NASA Center for AeroSpace Information, 301–621–0390.

12b. DISTRIBUTION CODE

13. ABSTRACT ***(Maximum 200 words)***

The NASA Vision for Space Exploration is focused on the return of astronauts to the Moon. While navigation systems have already been proven in the Apollo missions to the moon, the current exploration compaign will involve more extensive and extended missions requiring new concepts for lunar navigation. In this document, the results of an autonomous navigation error propagation assessment are provided. The analysis is intended to be the baseline error propagation analysis for which Earth-based and Lunar-based radiometric data are added to compare these different architecture schemes, and quantify the benefits of an integrated approach, in how they can handle lunar surface mobility applications when near the Lunar South pole or on the Lunar Farside.

14. SUBJECT TERMS

Moon; Navigation; Surface navigation; Positioning; Autonomous navigation

15. NUMBER OF PAGES

15

16. PRICE CODE

17. SECURITY CLASSIFICATION OF REPORT	18. SECURITY CLASSIFICATION OF THIS PAGE	19. SECURITY CLASSIFICATION OF ABSTRACT	20. LIMITATION OF ABSTRACT
Unclassified	Unclassified	Unclassified	